Ligand-Field-Dependent Behavior of Meta-GGA Exchange in Transition-Metal Complex Spin-State Ordering

Citation: Ioannidis, Efthymios I., and Kulik, Heather J. "Ligand-Field-Dependent Behavior of Meta-GGA Exchange in Transition-Metal Complex Spin-State Ordering." The Journal of Physical Chemistry A 121, 4 (January 2017): 874–884 © 2017 American Chemical Society

As Published: http://dx.doi.org/10.1021/acs.jpca.6b11930

Publisher: American Chemical Society (ACS)

Persistent URL: http://hdl.handle.net/1721.1/113022

Version: Author's final manuscript: final author's manuscript post peer review, without publisher's formatting or copy editing

Ligand-Field-Dependent Behavior of meta-GGA Exchange in Transition-Metal Complex Spin-State Ordering

Efthymios I. Ioannidis[1] and Heather J. Kulik[1,*]

[1]*Department of Chemical Engineering, Massachusetts Institute of Technology, Cambridge, MA 02139*

ABSTRACT: Prediction of spin-state ordering in transition metal complexes is essential for understanding catalytic activity and designing functional materials. Semi-local approximations in density functional theory, such as the generalized-gradient approximation (GGA), suffer from several errors notably including delocalization error that give rise to systematic bias for more covalently bound low-spin electronic states. Incorporation of exact exchange is known to counteract this bias, instead favoring high-spin states, in a manner that has recently been identified to be ligand-field dependent. In this work, we introduce a tuning strategy to identify the effect of incorporating the Laplacian of the density (i.e., a meta-GGA) in exchange on spin-state ordering. We employ a diverse test set of M(II) and M(III) first-row transition metal ions from Ti to Cu as well as octahedral complexes of these ions with ligands of increasing field strength (i.e., H_2O, NH_3, and CO). We show that the sensitivity of spin-state ordering to meta-GGA exchange is highly ligand-field dependent, stabilizing high-spin states in strong-field (i.e., CO) cases and stabilizing low-spin states in weak-field (i.e., H_2O, NH_3, and isolated ions) cases. This diverging behavior leads to generally improved treatment of isolated ions and strong field complexes over a standard GGA but worsened treatment for the hexa-aqua or hexa-ammine complexes. These observations highlight the sensitivity of functional performance to subtle changes in chemical bonding.

1. Introduction

The accurate description of transition metal chemical bonding, prediction of spin-state ordering, and evaluation of redox potentials are essential for the discovery of new materials (e.g., spin-crossover complexes[1-2]) and optimization of catalyst reactivity[3]. Approximate density functional theory (DFT) remains the method of choice for computational discovery[4-11], owing to its favorable balance of accuracy and efficiency.[12] Nevertheless, delocalization errors[13-14] and other biases in semi-local exchange approximations[15-16] (e.g., the generalized gradient approximation or GGA) produce systematic biases toward low-spin states[17-18] that prevent prediction of either qualitative (i.e., ground state identity) or quantitative (i.e., energetic splitting between states) spin-state properties. The bias toward low-spin states may be understood[19-20] by recalling the greater delocalization afforded through greater population of bonding orbitals in low-spin states than in high-spin states.

Conversely, incorporation of exact exchange in hybrid functionals, as developed in the context of Hartree-Fock (HF) theory, is well-known[18, 21-27] to reverse GGA low-spin bias[17-18, 22]. However, the strong chemistry-dependence of HF exchange effects on spin-state ordering[18, 21-22, 28] has motivated diverging proposals of either low[22, 29-31] or high[21, 32-33] HF exchange fractions in order to accurately predict transition metal complex properties. Explicit incorporation of exact exchange also remains computationally expensive in the context of periodic, plane-wave DFT. Given the growing interest in inorganic materials, such as metal-organic frameworks[34] and spin crossover materials[35-37], accurate prediction of spin-state ordering within pure DFT approximations is highly desirable. Current periodic studies rely on approximate delocalization error correction through the so-called DFT+U approach[38-40], which we have shown to yield accurate spin-state ordering in a range of molecular systems.[41-43] However, disadvantages for

DFT+U remain in the fact that one must calculate[43-44] or tune the *U* parameter, which introduces empiricism. We have also shown that optimal *U* choice may be ambiguous, depending on whether one is aiming to reproduce accurate density properties[14], recover piecewise linearity[45], or reproduce spin-state ordering[41-43].

Within pure DFT, meta-GGAs are functionals that incorporate the Laplacian of the density or equivalently the kinetic energy density; this more flexible form holds broad promise for reducing delocalization error in an exchange-correlation approximation.[46] Contemporary meta-GGAs have already been put forward for their potential in predicting the energetic (i.e., spin-state ordering) and structural properties of transition metal complexes[47]. Heavily parameterized, pure meta-GGA functionals (e.g., the over-20-parameter functional M06-L[48]) have demonstrated particularly impressive spin-state ordering[18, 49] and thermochemistry[50] in transition metal complexes. Isomer energetics of transition metal oxide molecules[51] have been shown to be in equivalently good agreement with multi-reference wavefunction theory for both the TPSS[52] and M06-L[48] meta-GGAs. More recently introduced meta-GGA functionals (i.e., the strongly constrained and appropriately normed meta-GGA or SCAN[53]) have shown promise for bulk transition metal oxide polymorphs[54].

At the same time, ambiguity remains in understanding of the extent to which meta-GGA exchange improves predictions over those obtained with GGA exchange for transition metals. Widely employed scaling relations in catalysis on bulk transition metals have been shown to be equivalent between pure GGA and meta-GGA descriptions[55], and meta-GGAs have been shown to produce limited improvement over GGAs on bulk property predictions.[56] Furthermore, some reactivity studies have preferred the hybrid meta-GGAs and hybrid GGAs[57-59] over pure meta-GGAs, and others suggested no substantial improvement of the hybrid meta-GGA M06 for spin-

state ordering over traditional GGA hybrids.[60] Still others have recommended double hybrid functionals in order to reproduce spin-state ordering in iron complexes[61], found too-strong high-spin bias in heavily parameterized meta-GGAs[62], or suggested that at least a small amount of exchange (i.e., 10% as in TPSSh) is necessary for accurate spin-state prediction[63]. Other properties, such as geometries[64-65] or thermochemistry[66-67] have been demonstrated to be better predicted by pure or hybrid GGAs, respectively, than meta-GGAs. Thus, there is a clear need to isolate and identify the effect of few-parameter, meta-GGA exchange descriptions on the spin-state ordering of transition metal complexes.

In this work, we introduce and apply a strategy to continuously tune from GGA to meta-GGA descriptions of exchange in order to isolate the effect of meta-GGA exchange on spin-state ordering in first-row transition metal ions and complexes across the periodic table (i.e., from Ti to Cu) and with ligands of increasing field strength (i.e., H_2O, NH_3, and CO). This approach enables us to identify whether meta-GGA exchange corrects for systematic GGA functional low-spin biases in transition-metal complexes. The outline of the rest of the paper is as follows. In Sec. 2, we review exchange-correlation functional forms and our tuning strategy. Computational details are presented in Sec. 3. In Sec. 4, we discuss effects of meta-GGA exchange tuning on transition metal ions and complexes. Finally, we provide our conclusions in Sec. 5.

2. Theory and Approach

We investigate the effect of incorporation of meta-GGA exchange by introducing an exchange tuning procedure to connect between two closely related functionals, the PBE[68] GGA and the TPSS[52] meta-GGA. In both cases, the GGA or meta-GGA exchange is expressed as an enhancement factor over local density approximation (LDA) exchange:

$$E_X^{\mathrm{PBE/TPSS}}(\rho_\alpha,\rho_\beta) = \int \rho \epsilon_x^{\mathrm{UEG}}(\rho_\alpha,\rho_\beta) F_x^{\mathrm{PBE/TPSS}}(s)\, d\mathbf{r} \tag{1}$$

where $\epsilon_x^{\mathrm{UEG}}$ is the exchange energy potential of the uniform electron gas used in the LDA. In PBE, the additional contribution of the reduced density gradient is introduced via a GGA enhancement factor, F_x^{PBE}:

$$F_x^{\mathrm{PBE}} = 1 + \kappa - \frac{\kappa}{1 + \frac{\mu s^2}{\kappa}} \tag{2}$$

where κ and μ are non-empirical constants selected to recover the local-spin density linear response[69] and to satisfy the Lieb-Oxford bound[70], and $s=s(\rho,\nabla\rho)$ is a functional of the reduced density gradient.

The meta-GGA exchange-enhancement expression in the closely-related TPSS[52] functional was derived by satisfying all of the exact or nearly exact constraints satisfied by the PBE GGA plus 3 additional constraints[71] without introduction of empirical parameters. The TPSS meta-GGA exchange-enhancement factor, F_x^{TPSS}, is expressed as:

$$F_x^{\mathrm{TPSS}} = 1 + \kappa - \frac{\kappa}{1 + \frac{x}{\kappa}}\ , \tag{3}$$

where κ is the same constant as in eq. 2 and $x=x(\rho,\nabla\rho,\nabla^2\rho)$ is a functional of the electron density, the electron energy gradient, and the electron kinetic energy through the reduced Laplacian of the electron density, α.[52]

Thus, continuous tuning of the exchange-enhancement factors between the PBE and TPSS limits may be made by constructing a combined exchange enhancement factor where the pure gradient contribution is separated from the gradient-Laplacian contribution. Including an additional weighting factor, a_x, between the two contributions to exchange, this modified enhancement factor becomes:

$$F_x^{\mathrm{TPSS/PBE}} = 1 + \kappa - \frac{\kappa}{1 + \frac{a_x x + (1 - a_x)\mu s^2}{\kappa}} \tag{4}$$

In this work, we smoothly vary exchange from the PBE-GGA limit ($a_x \rightarrow 0$) to the TPSS meta-GGA limit ($a_x \rightarrow 1$) in order to reveal the role of meta-GGA exchange in spin-state ordering in an analogous fashion to previous exact exchange tuning studies[18, 21, 28, 72]. Comparisons of TPSS and PBE for spin state ordering have been made previously, but continuous variation introduced here provides new insight into the role of meta-GGA exchange. The exchange enhancement factor for intermediate values of a_x is a non-linear admixture of the PBE and the TPSS values (Figure 1). Identification of how exchange-enhancement evolves with PBE/TPSS mixing reveals the most substantial changes for small *s* and intermediate values of the reduced Laplacian, α. Correlation is treated with the TPSS functional in all cases in order to isolate the dominant exchange effect[18, 21, 28, 72] on spin-state ordering. The extent to which non-linearity in the exchange-enhancement factor also makes energetic predictions non-linear is limited and discussed in detail in sec. 4.

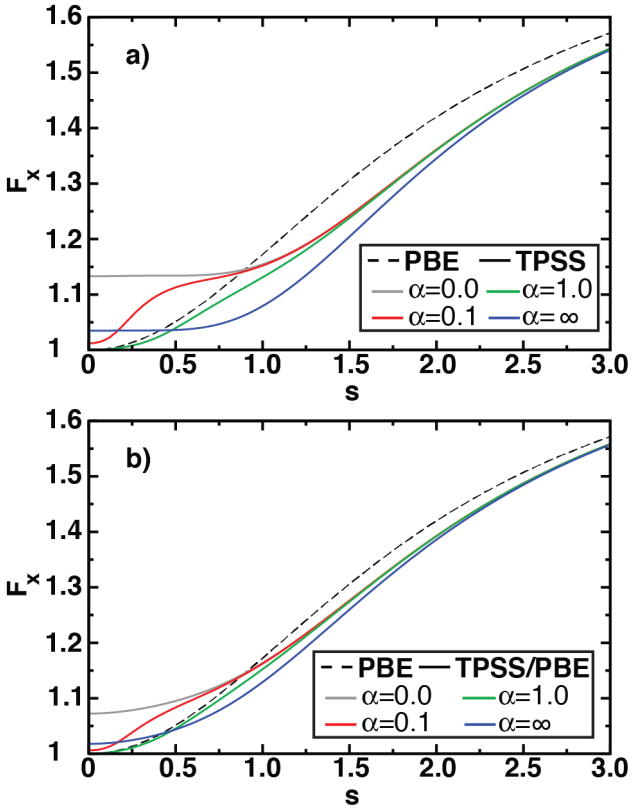

Figure 1. (a) TPSS (solid lines) and PBE (dashed line) enhancement factors, F_x, as functions of the reduced gradient s for four different values of the reduced kinetic energy, α. (b) TPSS/PBE (solid lines) and PBE (dashed line) enhancement factors, F_x, as functions of the reduced gradient, s, for four different values of the reduced kinetic energy, α, at a_x=0.5.

Functional tuning is carried out to compare the effect of exchange descriptions on the electronic energy adiabatic high-spin (HS)-low-spin (LS) state splittings:

$$\Delta E_{\text{HS-LS}} = E_{\text{HS}}(R_{\text{HS}}) - E_{\text{LS}}(R_{\text{LS}}) \ , \tag{5}$$

where $E_{\text{HS}}(R_{\text{HS}})$ or $E_{\text{LS}}(R_{\text{LS}})$ represent the energies of HS and LS states obtained at their ground state geometries, respectively. Comparisons between HS or LS states and intermediate spin states (IS) are evaluated in an equivalent manner. We neglect spin-state dependent vibrational and solvation effects that would be necessary if the goal were to compare to experimental spin-state

ordering.[17] We instead focus on how functionals tune electronic energies, in analogy to previous work on HF exchange tuning.[18, 21-22]

In order to reveal effects of functional tuning, we approximate the partial derivative of the relative electronic energy between HS and LS states ($\Delta E_{\text{HS-LS}}$) with respect to meta-GGA exchange fraction, a_x, with a linear regression fit:

$$\frac{\Delta\Delta E_{\text{HS-LS}}}{\Delta a_x} \approx \frac{\partial \Delta E_{\text{HS-LS}}}{\partial a_x} \quad , \tag{6}$$

where we denote $\frac{\partial \Delta E_{\text{HS-LS}}}{\partial a_x}$ the meta-GGA exchange sensitivity of spin-state splitting. We introduce the notation MGGAX, a single unit of which corresponds to the range from a_x= 0 (0%) a_x= 1 (100%) meta-GGA exchange, and the units of meta-GGA exchange sensitivity, $\frac{\partial \Delta E_{\text{HS-LS}}}{\partial a_x}$, that we use are kcal/mol per MGGAX. In the case of transition-metal complexes, any effect of functional tuning on the preferred geometry is also incorporated into the spin-state ordering.

3. Computational Details

Spin-state orderings of atoms and transition metal-complexes were evaluated with the meta-GGA tuning strategy outlined in sec. 2 (structures shown in Figure 2).

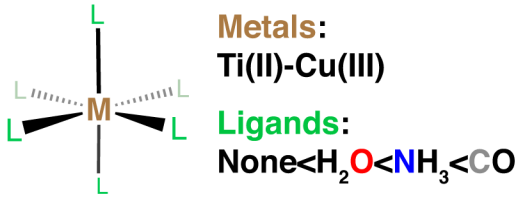

Figure 2. Summary of octahedral complexes studied in this work with M(II) and M(III) metals from Ti(II) to Cu(III) inclusive and isolated atoms (ligand = None) as well as ligands of increasing ligand field strength: water, ammonia, and carbon monoxide.

Spin-state ordering was evaluated for each transition metal ion in +2 (Ti-Ni) and +3 (V-Cu) oxidation states. The electron configuration of all these ions is nominally $3d^x4s^0$, where x ranges from 2 to 8 (Table 1). Reference data from the National Institute of Standards and Technology (NIST) database[73] was used to identify relevant spin states for comparison and for evaluation of exchange-correlation functional errors (Table 1). The lowest energy state of each spin multiplicity was identified in all cases, leading to a single high-spin and low-spin definition for all ions except for the d^4-d^6 cases (i.e., Cr(II), Mn(II/III), Fe(II/III), and Co(III), see Table 1), which also had low-energy intermediate spin states. The meta-GGA-tuned energies were obtained using the GAMESS-US[74] code spanning 0% meta-GGA (i.e., GGA) to 100% meta-GGA in 25% increments. Calculations employed Dunning's augmented correlation consistent triple-ζ basis set[75] (aug-cc-pVTZ). GAMESS by default increases radial grid fidelity when meta-GGA calculations are employed. This higher grid density was also employed for the pure GGA calculations. For the ions, the electronic state was selected by visual assessment, including from restricted and unrestricted singlet candidates, in order to obtain states corresponding to the experimental term symbol of the isolated atom. For all unrestricted calculations, the default values for level shifting and convergence tolerance ($1x10^{-5}$ a.u.) were used.

Table 1. Spin-states for ions in M(II) and M(III) oxidation states with corresponding electron configurations and experimental relative energies (in kcal/mol) from the NIST[73] atomic spectra database database for the 8 first-row transition metal ions studied in this work.

	M(II)			M(III)		
Element	HS	LS	IS	HS	LS	IS
Ti ($3d^2$/--)	triplet	singlet	--	--	--	--
	0.00	24.2	--	--	--	--
V($3d^3$/$3d^2$)	quartet	doublet	--	triplet	singlet	--
	0.00	34.1	--	0.00	31.4	--
Cr($3d^4$/$3d^3$)	quintet	singlet	triplet	quartet	doublet	--
	0.00	71.9	48.0	0.00	43.1	--
Mn($3d^5$/$3d^4$)	sextet	doublet	quartet	quintet	singlet	triplet
	0.00	111.8	76.6	0.00	--	59.0

Fe($3d^6$/$3d^5$)	quintet	singlet	triplet	sextet	doublet	quartet
	0.00	86.7	55.3	0.00	134.4	92.0
Co($3d^7$/$3d^6$)	quartet	doublet	--	quintet	singlet	triplet
	0.00	48.4	--	0.00	102.6	65.3
Ni($3d^8$/$3d^7$)	triplet	singlet	--	quartet	doublet	--
	0.00	39.9	--	0.00	56.7	--
Cu(--/$3d^8$)	--	--	--	triplet	singlet	--
	--	--	--	0.00	46.4	--

Octahedral transition metal complexes were studied with representative weak-field (H_2O, NH_3) and strong-field (CO) ligands (Figure 2). The selected spin-states for these complexes were the HS and LS states identified for transition metal ions based on comparison of data available from NIST[73] (Table 1). The sole exception to this assignment is that the singlet Mn(III) ion energy was not available from the same NIST database[73], but we define a singlet state as the low-spin state for the Mn(III) complexes. Structures and input files for these calculations were generated using molSimplify[76], a recently introduced toolkit for automating simulation of transition metal complexes. The molSimplify[76] code uses trained metal-ligand bond lengths and force-field pre-optimization to provide good initial guesses for DFT geometry optimizations. We carried out exchange tuning from 0% to 100% meta-GGA exchange in 10% increments to ensure a consistent electronic state was smoothly converged. Initial geometry optimizations in GAMESS were performed with the 6-31G*[77] basis set. All optimized geometries and a list of the select complexes that did not converge are provided in the Supporting Information). The spin-state ordering of these complexes were obtained from single point energy calculations using the larger triple-ζ def2-TZVP[78] basis set.

Convergence difficulties for one of the two spin states prevented study of exchange tuning on select complexes ($[Ni(CO)_6]^{3+}$, $[Mn(NH_3)_6]^{3+}$, $[Ni(NH_3)_6]^{3+}$, $[Cu(H_2O)_6]^{3+}$), as indicated in the Supporting Information. In particular, Jahn-Teller distortion that leads to dissociation of

axial ligands was problematic for the low-spin, doublet Ni(III) carbonyl or ammine complexes, low-spin, singlet Cu(III) hexa-aqua complexes, and high-spin, quintet Mn(III) ammine complexes. Default values were used for level shifting and the convergence criteria were set to $1x10^{-4}$ a.u./bohr for the gradient in geometry optimizations and to a 10^{-6} a.u. change in the density matrix between iterations for convergence of the self-consistent field calculation. Partial charges were obtained from the GAMESS interface with the Natural Bond Orbital (NBO) v6.0 package[79]. Consistent electronic states were obtained as exchange-mixing was varied through trial-and-error restarts from converged guesses where necessary. The consistency was validated by ensuring smooth variation of total energies, S^2 values, and orbital occupancies with NBO. Analysis of the density at bond critical points (BCPs[80]) was performed using the Multiwfn post-processing package.[81]

Complete active space second-order perturbation theory (CASPT2)[82] calculations were performed with Molcas 8.0[83] on $[Fe(NH_3)_6]^{2+}$ due to the lack of recent literature CASPT2 data for this complex. Relativistic atomic natural orbital (ANO-rcc) basis sets[84-85] contracted to [7*s*6*p*5*d*3*f*2*g*1*h*] for Fe, [4*s*3*p*2*d*1*f*] for N and [3*s*1*p*] for H were used together with the scalar-relativistic Douglas-Kroll Hamiltonian[86-87]. An imaginary level shift of 0.1 and IPEA shift of 0.25 were used[88-89] with an active space of 10 electrons in 12 orbitals.

4. Results and Discussion

4a. Atomic Spin State Ordering

Semi-local GGA functionals are well-known[18, 21-22] to have strong preference for low-spin states over high-spin states in transition metal complexes due to differences in delocalization[14, 19] between high- and low-spin complexes, and incorporation of HF exchange reverses this

preference[18, 21-22]. However, for weak-field ligands (e.g., water) the extent of delocalization may be limited[45], and underlying biases in the functional for energetics of the transition metal ion become important. Thus, as a limiting case, we evaluate the spin-state energetics for M(II) and M(III) first-row transition metal ions and compare to reference experimental data (Table 1) to identify biases in semi-local GGA and meta-GGA calculations (Supporting Information Tables S1-S14).

Experimentally, high-spin (HS) states are universally preferred by as much as 5.83 eV (i.e., 134 kcal/mol) over low-spin (LS) counterparts (i.e., for Fe(III) sextet versus doublet states). Mid-row Cr(II) through Co(III) have a third accessible intermediate-spin (IS) state that generally is also intermediate in energetics between the HS and LS spin states. The smallest HS-LS splitting is observed for the $3d^2$ Ti(II) triplet-singlet gap at 1.05 eV (i.e., 24 kcal/mol). Isolating comparisons to the most closed-shell spin state and a higher-spin state that differs by unpairing of only one pair of electrons (i.e., the only two states for early and late transition metals, the two lowest spin states for the mid-row transition metals) reveals an oscillating but increasing energetic penalty for this pairing from as low as 1.05 eV (i.e., 24 kcal/mol) in Ti(II) singlet-triplet to as high as 2.46 eV for Ni(III) doublet-quartet or 2.01 eV for Cu(III) singlet-triplet (i.e., 46-56 kcal/mol).

GGA spin-state splitting ΔE_{HS-LS} errors may be grouped into primarily positive values for early or late transition metals and negative values for the mid-row transition metals (saturated lines in Figure 3). Evaluation of GGA spin-state splittings for the two spin-state early- (Ti(II), V(III/II), Cr(III)) and late- (Co(II), Ni(III/II), and Cu(III)) transition metal ions reveals that GGA exchange consistently understabilizes the high-spin states of these ions (black circles in Figure 3). This low-spin stabilization error grows from as little as 10 kcal/mol in Ti(II) to as much as 30

kcal/mol in Ni(II). Recalling the shift in spin-state energetics experimentally from 24 to 46-56 kcal/mol, it becomes apparent that nearly constant estimation of pairing energetics by the GGA will produce increasing errors as the *d* shell is filled. Incorporation of meta-GGA exchange has a weakly favorable effect for Ti(II), V(III), Ni(III), Ni(II), and Cu(III), reducing errors by 1-3 kcal/mol by slightly stabilizing the HS state over the GGA HS-LS splitting (see Supporting Information Tables S1-S14). Conversely, V(II), Cr(III), and Co(II) HS states are further destabilized by incorporation of a meta-GGA, worsening errors by as much as an additional 6 kcal/mol (Cr(III)). Thus, for the single pair of electron differences in nearly closed shell early- or late-transition metal ions, meta-GGA exchange both lacks the consistent behavior of HF exchange (i.e., to correct GGA LS bias) and also appears to have a relatively small effect (2-5 kcal/mol) in comparison to the magnitude of GGA errors (up to 30 kcal/mol).

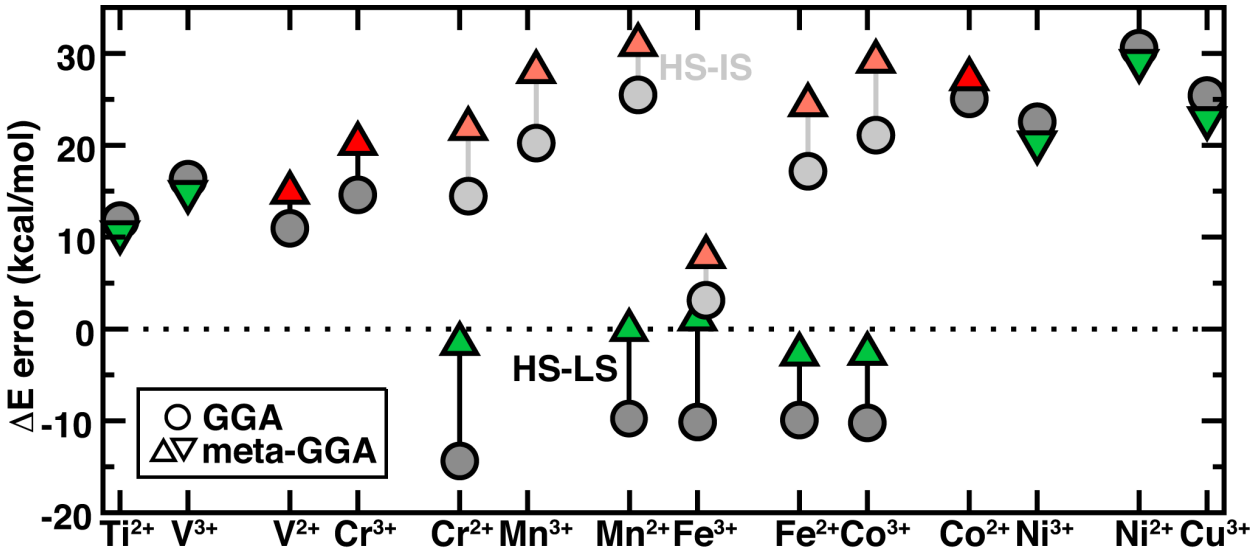

Figure 3. GGA (gray filled circles) and meta-GGA (up or down triangles) error in spin-state ordering, ΔE, of first-row transition metal ions with respect to experimental references in kcal/mol for both high-spin to low-spin ordering (HS-LS, shown in black lines and saturated symbols) and high-spin to intermediate-spin ordering (HS-IS, shown in gray lines and unsaturated symbols). The zero error point is shown as a dotted line. The meta-GGA symbols are filled red or green if the error is increased or decreased with respect to GGA, respectively. Up

triangles are chosen for cases where the ΔE becomes less biased toward the higher spin state, and down triangles are shown for the opposite.

Behavior of both GGAs and meta-GGAs is reversed in the mid-row transition metals where HS-LS splitting corresponds to comparison of states that differ by unpairing of four electrons: from the quintet-singlet states of d^4 Cr(II) to d^6 Co(III). The GGA functional systematically overstabilizes the HS with respect to the LS by as much as around 18 kcal/mol (gray circles in Figure 3). This HS stabilization by GGA diverges from expectations on the basis of transition metal complexes and with the trends in the early- and late- transition metals. This difference can be understood through the states being compared: in the mid-row transition metals HS-LS corresponds to a difference in pairing for four electrons, whereas in the early- and late-transition metals, this difference is only for a single pair of electrons. Comparison of HS-IS splitting in the mid-row transition-metals to early- or late- transition metals reveals more comparable trends in HS destabilization. In the mid-row HS-LS spin-state orderings, addition of meta-GGA exchange dramatically reduces errors with respect to experimental references (green triangles in Figure 3). By shifting HS-LS splittings by between 8 and 12 kcal/mol, full meta-GGA exchange predicts the HS-LS splitting for all cases within 1-2 kcal/mol of the experimental value. Thus, on the basis of HS-LS spin-state ordering of transition metal ions, meta-GGA exchange provides substantial improvement over a standard GGA description.

In the mid-row cases, we may also consider HS-IS ordering energetics with GGA (light gray circles in Figure 3). From Cr(II) to Mn(II), HS-IS spin-state errors increase from around 12 to 25 kcal/mol, decreasing to 2 kcal/mol for sextet-quartet ordering of d^5 Fe(III) but then increasing again in Fe(II) and Co(II). Overall, the HS state is generally destabilized with respect to the IS state in comparison to experimental reference by GGA by an amount that increases with

increasing *d* configuration until abruptly decreasing when the shell is half-filled before increasing again. Here, it is less clear if any experimental increase in HS-IS splitting is underlying the increase in GGA errors. In all of these cases, incorporation of meta-GGA exchange leads to further destabilization of the HS state, by a consistent amount around 6-10 kcal/mol per ion that increases meta-GGA errors over GGA errors with respect to the experimental reference by the same amount (light red triangles in Figure 3). Put another way, meta-GGA exchange corrects midrow HS-LS splitting but overstabilizes intermediate spin-states, pushing them too close to the HS state and too far below the LS state. The near constant error suggests limited dependence of the functional behavior on *d* shell filling. The HS-IS behavior of Cr(II)-Co(III) is roughly consistent with the most-intermediately filled early- and late-row cases (i.e., V(II), Cr(III), and Co(II)), suggesting some systematic errors in GGAs that are worsened by meta-GGAs in transition metal ions.

Overall mean absolute errors (MAEs) for HS-LS splittings on the transition metal ions with meta-GGA exchange (12.9 kcal/mol) are reduced with respect to GGA values (16.3 kcal/mol) by nearly 4 kcal/mol (Table 2). The recently introduced[53] SCAN functional performs comparably to the TPSS meta-GGA exchange functional on transition metal ions with mean absolute errors in HS-LS splitting around 15 kcal/mol (Supporting Information Table S15). The reduction in only the HS-LS error in the midrow transition metal ions is even more substantial with a reduction in GGA MAE from 10.7 kcal/mol to 1.7 kcal/mol for meta-GGAs. Maximum absolute errors are also reduced from 14.6 kcal/mol for GGA to 2.8 kcal/mol for HS-LS splittings of midrow atoms with meta-GGAs.

Table 2. Mean absolute error and maximum error in spin-state splitting (in kcal/mol) for high-spin/low-spin ordering (HS-LS) of all transition metal ions (HS-LS all), the midrow subset from Cr(II) to Co(III) (HS-LS midrow), and the high-spin/intermediate-spin ordering (HS-IS) of the midrow subset from Cr(II) to Co(III). GGA exchange is compared to meta-GGA exchange.

Ordering	GGA	meta-GGA
HS-LS all	16.3 (30.6)	12.9 (29.1)
HS-LS midrow	10.9 (14.6)	1.7 (2.8)
HS-IS midrow	16.9 (25.5)	23.7 (30.9)

However, this improvement comes at the cost of worsening HS-IS spin-state splitting MAEs from 16.9 to 23.7 kcal/mol and maximum absolute error from 25.5 kcal/mol to 30.9 kcal/mol, for GGA to meta-GGA, respectively. The majority of improvements made by incorporation of meta-GGA exchange come from destabilization of HS states in cases where the GGA already overstabilizes HS states. At the same time, some early- and late-transition metals have spin-state orderings weakly improved by incorporating meta-GGA exchange that leads to HS stabilization, suggesting flexibility in the manner in which meta-GGA exchange alters spin-state ordering. In contrast, HF exchange systematically stabilizes HS states, and its incorporation to correct spin-state ordering is reliant upon the assumption that GGA only overstabilizes LS states, which does not apparently hold in the case of mid-row transition metal ions.

4b. Transition Metal Complex Spin-State Ordering

Systematic low-spin bias for GGA functionals is known in octahedral transition metal complexes, but the effect of meta-GGA exchange is not well-established. We now consider the effect of meta-GGA exchange on octahedral transition metal complexes with increasingly strong field ligands (i.e., H_2O to NH_3 to CO, see Figure 2). It is worthwhile to note that various pure meta-GGA functionals may perform differently due to differences in parameterization. A comparison of HS-LS errors for Fe(II) octahedral complexes and ions as determined against

correlated wavefunction theory reference[90-92] reveals comparable performance for TPSS[52] and SCAN[53] but improved spin-state ordering with the more highly-parameterized M06-L functional[48] (Supporting Information Table S16). We focus our evaluation to TPSS due to the straightforward tuning of the enhancement factor not possible with the other two meta-GGA functional forms (see sec. 2), and we now identify the effect of meta-GGA exchange across a range of transition metal complexes with varying electron configuration and ligand field strength (Supporting Information Tables S17-S54). We anticipate that the previously noted comparable performance of SCAN and TPSS on Fe(II) complexes may make observations made here using TPSS tuning transferable to more recently developed meta-GGA functionals as well.

For transition metal ions, the most substantial meta-GGA exchange sensitivity was observed for mid-row transition metal ions (see sec. 4a). Thus, we compare meta-GGA exchange sensitivity for the Fe(III) ion and $[FeL_6]^{3+}$ d^5 complexes where L=H_2O, NH_3, or CO over the range of 0% meta-GGA exchange to 100% meta-GGA exchange (Figure 4). The Fe(III) transition-metal complex sensitivity is reduced with respect to the isolated ion. Both hexa-aqua and hexa-ammine complexes have HS states that are destabilized with increasing meta-GGA exchange by around 9 kcal/mol and 5 kcal/mol over the range of meta-GGA exchange versus 11 kcal/mol for the ion. Conversely the hexa-carbonyl complex HS state is stabilized with increasing meta-GGA exchange by around -4 kcal/mol over the range of meta-GGA exchange. These observations are preserved for Fe(II) ions and transition metal complexes, with slightly smaller differences between the isolated ion, hexa-aqua, and hexa-ammine complexes but a significant reversal in trend for the carbonyl complex in comparison to the weaker-field complexes (Figure 4).

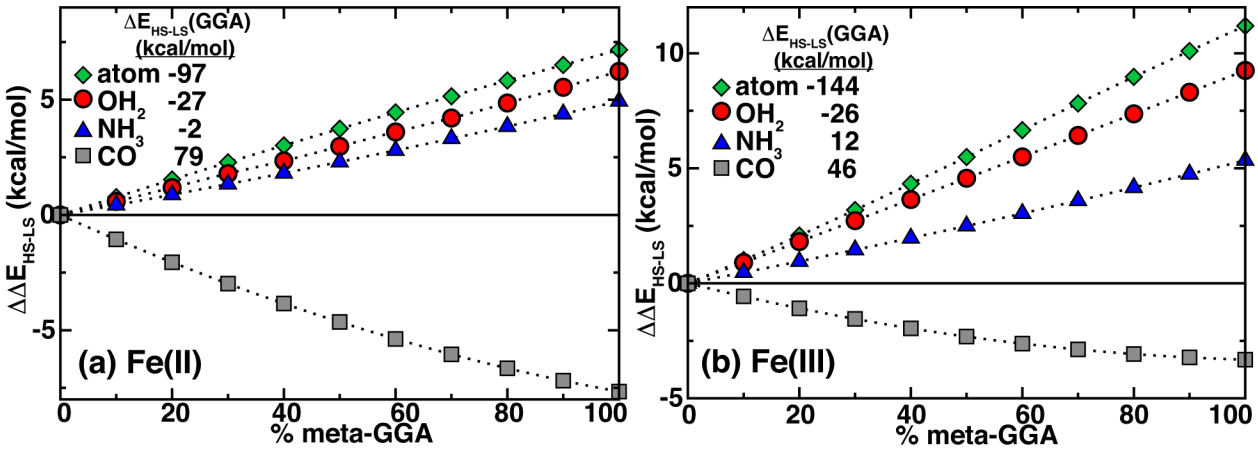

Figure 4. Shift of spin-state splitting, ΔE_{HS-LS}, with percentage of meta-GGA exchange in Fe ion (green diamonds), hexa-aqua iron (red circles), hexa-ammine iron (blue triangles), and hexa-carbonyl iron (gray squares) in kcal/mol for (a) Fe(II) and (b) Fe(III) oxidation states. The GGA exchange splitting (in kcal/mol) is indicated in the inset, to facilitate alignment of the ΔE_{HS-LS} values to zero at the 0% meta-GGA (i.e., GGA exchange) value. Both Fe(II) and Fe(III) graphs span the same 17 kcal/mol range.

In comparing these four cases, we observe ligand-field dependence of meta-GGA exchange contributions to HS-LS splitting. The strongest field ligands have considerable covalent bonding that is enhanced in the LS state over the HS state, and the enhanced covalency is apparently weakly penalized upon incorporation of meta-GGA exchange. This less pronounced effect is counterbalanced by the effects described earlier for ions in the other three cases, leading to HS destabilization. A comparison of the HS and LS densities between the $[Fe(CO)_6]^{3+}$ and $[Fe(OH_2)_6]^{3+}$ complexes highlights the covalent bonding origins of the difference in meta-GGA exchange behavior (Figure 5). Strong delocalization in the Fe-C bond is apparent for LS $[Fe(CO)_6]^{3+}$ but absent from the HS state. Weak, nearly equivalent delocalization is observed in both the HS and LS states of the $[Fe(OH_2)_6]^{3+}$ complex, with both cases qualitatively residing between the HS and LS carbonyl cases. Comparable trends for hybridization are observed for Fe(II) hexa-aqua and hexa-carbonyl complexes as well (Supporting Information Figure S1). It thus appears based on review of trends in these Fe complexes that meta-GGA

exchange will counteract this bias somewhat in strongly-covalent complexes but worsen behavior for cases with decreased hybridization.

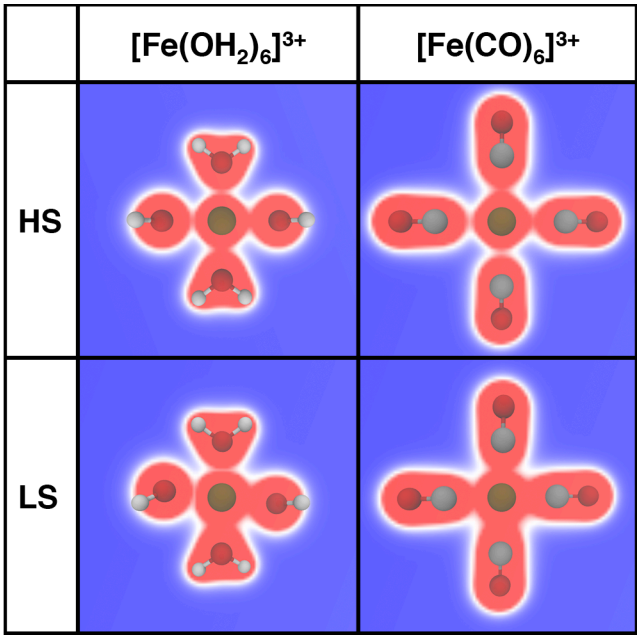

Figure 5. Cuts of the total electron density in the equatorial plane of $[Fe(OH_2)_6]^{3+}$ (left) and $[Fe(CO)_6]^{3+}$ right in high-spin (top) and low-spin (bottom) configurations. The white border indicates an isosurface of 0.06 e, red shading indicates density values higher than that isosurface value, and blue density values below that isosurface value. Iron atoms (brown), carbon atoms (gray), oxygen atoms (red), and hydrogen atoms (white) in the equatorial plane are shown as balls and sticks.

Comparisons of meta-GGA exchange sensitivity for octahedral complexes across the periodic table to the previously characterized transition metal ions reveals consistent behavior with the Fe(III) cases (Figure 6). Overall positive meta-GGA exchange sensitivities of the HS-LS splitting for weak-field hexa-aqua and hexa-ammine complexes track with but are slightly smaller than the values observed for the isolated ions. For the transition-metal complexes, a variable degree of unrestricted character was observed (Supporting Information Table S55). In order to facilitate comparison between meta-GGA behavior in isolated ions and transition metal complexes, we also report Mn^{3+} data, excluded from sec. 4a due to the absence of accurate experimental reference data for the singlet Mn^{3+} ion. Comparable behavior is observed for the two weak-field ligands and the isolated ions, with the highest positive meta-GGA exchange

sensitivity occurring for the mid-row transition metals, at about 10 kcal/mol over the range of meta-GGA exchange for the complexes. Examination of the early- and late- transition metals reveals further reduced meta-GGA exchange sensitivity compared to the ions, with sensitivities below 2 kcal/mol per MGGAX and limited discernible trend in sign for both early Ti(II), V(III/II), Cr(III) and late Ni(III/II), Cu(III) complexes.

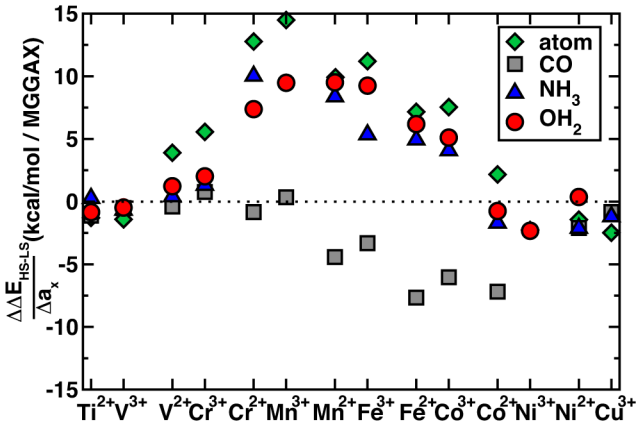

Figure 6. The approximate partial derivative, of spin-state splitting, ΔE_{HS-LS}, with meta-GGA exchange, a_x, in kcal/mol per unit of meta-GGA exchange (MGGAX) for Ti^{2+} to Cu^{3+} as isolated ions (green diamonds) and in octahedral +2 or +3 ML_6 complexes with L=CO (gray squares), L=NH_3 (blue triangles), and L=OH_2 (red circles).

Conversely, strong-field hexa-carbonyl complexes of midrow transition metals have negative meta-GGA exchange sensitivity, stabilizing HS states to an increasing degree from d^4 Cr(II) to d^7 Co(II). Magnitudes of this stabilization are at most around 8 kcal/mol per MGGAX for iron and cobalt complexes. We have computed the effect of meta-GGA exchange on $[Fe(PH_3)_6]^{2+}$ and $[Fe(PH_3]_6]^{3+}$ complexes in order to confirm that our ligand field observation is valid beyond the carbonyl complexes alone. Indeed, both the $[Fe(PH_3)_6]^{2+}$ and $[Fe(PH_3]_6]^{3+}$ complexes exhibit negative meta-GGA exchange sensitivities of -4.7 kcal/mol and -1.0 kcal/mol, respectively (Supporting Information Tables S56-S7).

The GGA HS-LS spin-state splitting may be used as an estimate of the DFT metal-centric spectrochemical series and thus used to differentiate trends in meta-GGA exchange sensitivities

across the periodic table. The manganese, iron, and cobalt hexa-carbonyl complexes generally have the largest HS-LS splitting and also the most negative HS-LS exchange sensitivities (Supporting Information Figures S2-S3). In each of these cases, the difference between HS and LS electron configurations corresponds to population of two (for d^5-d^6) or one (for d^7) additional high-energy e_g states in the HS case over the lower-energy t_{2g} states. The greater delocalization of the density afforded by the t_{2g} states with ligand states leads to GGA preference for the LS state. Conversely, the incorporation of meta-GGA exchange stabilizes these HS states, where it has little effect on early or late transition metals with low spin-state splitting due to comparable orbital populations between both spin states. Thus, this aspect of meta-GGA exchange is highly desirable: it counteracts HS destabilization proportionally for the cases where GGA is likely most strongly biased against the HS state.

The HS-LS splitting dependence of meta-GGA exchange sensitivity is mostly preserved for the weaker field ligands but is not as monotonic, particularly for hexa-ammine complexes (Supporting Information Figures S4-S7). Overall good correlations are observed for meta-GGA exchange sensitivity with spin-state splitting across a range of metals and ligand types, suggesting that the GGA HS-LS splitting alone can provide a suitable guide to the expected influence of inclusion of meta-GGA exchange on spin-state ordering (Supporting Information Figures S8-S9). Other proxies for differences in covalent bonding and delocalization in the HS and LS state that we have previously found beneficial include the difference in metal-centered partial charge between the HS and LS states[14, 18] and the exchange sensitivity of this partial charge difference.[18] Both of these metrics correlate well with meta-GGA exchange sensitivity: i) higher charge differences correspond to more negative exchange sensitivity (Supporting Information Figures S10-S11) and ii) increasingly negative charge sensitivities with meta-GGA

exchange (i.e., increasingly comparable charges between HS-LS states) yield more positive meta-GGA HS-LS sensitivities (Supporting Information Figure S12 and Table S58). Finally, bond-centric metrics that more directly probe covalency such as the difference in density at the bond critical points and the Laplacian of the density at the bond critical point both correlate well to meta-GGA exchange sensitivities (Supporting Information Figures S13-S14 and Text S1). Overall, knowledge of the chemical bonding in the systems of interest provides guidance of whether meta-GGA exchange will have a HS-stabilizing or HS-destabilizing effect on spin-state ordering.

4c. Combining HF and meta-GGA exchange

Many meta-GGA exchange-correlation functionals are developed with an admixture of Hartree-Fock exchange. We[18] and others[21] have investigated the strongly linearly HS-favoring effect of HF exchange on spin-state ordering in transition metal complexes that appears to counteract pure GGA LS bias. We now assess the combined influence of HF and meta-GGA exchange on representative strong-field, $[Fe(CO)_6]^{2+}$ and weak-field, $[Fe(II)(NH_3)_6]^{2+}$ cases. In order to simultaneously tune both, we describe their composite effect as:

$$\Delta E_{HS\text{-}LS} = \Delta E^{GGA}_{HS\text{-}LS} + \frac{\Delta\Delta E_{HS\text{-}LS}}{\Delta a_x} a_x + \frac{\Delta\Delta E_{HS\text{-}LS}}{\Delta a_{HF}} a_{HF} \quad , \qquad (7)$$

where $\Delta E^{GGA}_{HS\text{-}LS}$ is the spin-state splitting calculated at 0% HF exchange with modB3LYP[18], the second term is the meta-GGA exchange sensitivity previously described, $\frac{\Delta\Delta E_{HS\text{-}LS}}{\Delta a_{HF}}$ is the approximate partial derivative of the splitting with respect to HF exchange, and a_{HF} the fraction of HF exchange. Nearly linear behavior for separate tuning of these two quantities motivates this composite approximation. We compare this composite spin-state splitting approximated at any

percentage of HF or meta-GGA exchange to literature benchmark values calculated with complete active space perturbation theory (CASPT2) references[92-93] (Figure 7).

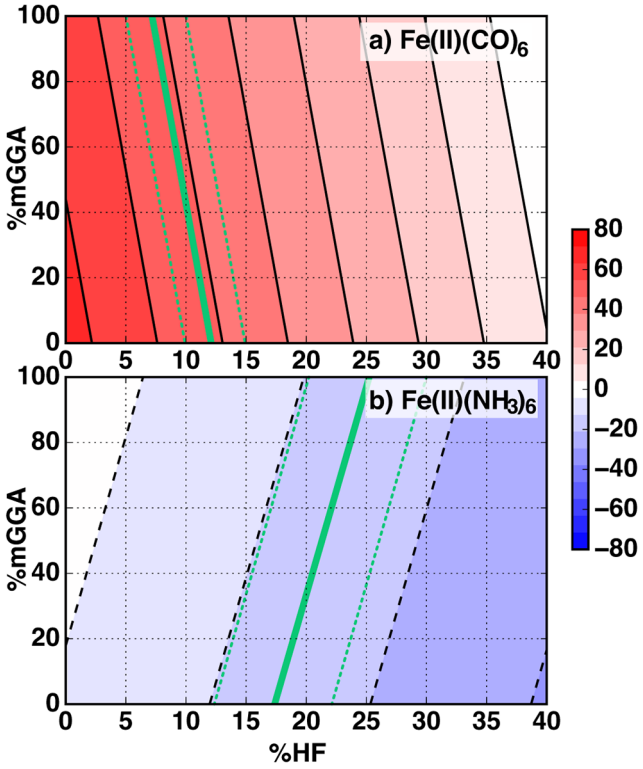

Figure 7. Spin-state splitting, $\Delta E_{HS\text{-}LS}$, in kcal/mol as a function of % HF exchange (%HF, *x*-axis) and % meta-GGA exchange (%mGGA, *y*-axis) included for $Fe(II)(CO)_6$ (top) and $Fe(II)(NH_3)_6$ (bottom). Agreement with benchmark or our own CASPT2 values[93] is indicated with a green solid line along with a ±3 kcal/mol confidence interval (green dotted lines) in both cases. The spin-state splitting plane is colored according to the colorbar shown in inset, and dashed or solid lines correspond to increments of 10 kcal/mol.

Consistent with our reported meta-GGA exchange sensitivities (sec. 4b) and previously reported HF exchange sensitivities[18], we observe stronger dependence of spin-state splitting on HF exchange than meta-GGA exchange. For $[Fe(CO)_6]^{2+}$, $\Delta E_{HS\text{-}LS}$ decreases by around 60 kcal/mol over the range of 0-40% HF exchange that is typically used in hybrid functionals but only by around 8 kcal/mol over the range of 0-100% meta-GGA exchange. The synergistic effect of meta-GGA and HF exchange on the spin-state splitting of $[Fe(CO)_6]^{2+}$ indicates that in this case incorporation of meta-GGA exchange decreases the amount of HF exchange required from

12% to 7% to reach quantitative agreement with CASPT2 (Figure 7a). This reduction suggests that meta-GGA exchange may be incorporated to improve electronic structure characterization of strong-field ligands, without any explicit treatment of HF exchange, a potentially useful approach for reducing computational cost in plane-wave calculations, or, alternatively, at low HF exchange fractions, as in TPSSh[94] in localized basis set codes.

Combined meta-GGA and HF tuning trends differ on the weak-field $[Fe(NH_3)_6]^{2+}$. For $[Fe(NH_3)_6]^{2+}$, HF and meta-GGA exchange have opposing effects on $\Delta E_{HS\text{-}LS}$, with a HS-LS splitting decrease of 25 kcal/mol observed over the range 0-40% HF exchange, whereas including full meta-GGA exchange increases this spin state splitting by 5 kcal/mol. Thus, an HF exchange ratio of 17% needed for the GGA hybrid to reach quantitative agreement with CASPT2 is increased to 25% by inclusion of meta-GGA exchange (Figure 7b). The higher HF exchange ratio needed for weak field ligands is likely due to our earlier observations[18] of decreased HF exchange-sensitivity of HS-LS splittings for weaker field ligands. Here, the opposing effect of meta-GGA exchange reduces the already lower efficiency of HF exchange tuning even further. The different amounts of required HF exchange observed in our data are consistent with the literature where arguments for both high[21, 32-33] and low[22, 29-30] percentages of included HF exchange have been proposed in conjunction with either GGA[95-97] or meta-GGA[98-101] functionals for the description of transition metal complexes.

Indeed, in the weak field limit of isolated ions, we observe HF exchange to have a much more modest effect on spin-state ordering (Table 3). HF exchange universally favors high-spin states but by less than 10 kcal/mol from 0% to 100% HF exchange on transition metal ions. For early- and late-row transition metal ions Ti(III) and Ni(II), incorporation of HF exchange is beneficial in partially correcting GGA bias, where the incorporation of meta-GGA exchange

alone is insufficient. For Fe(II) ion, on the other hand, meta-GGA exchange corrects a high-spin bias, and incorporation of any fraction of HF exchange counteracts this beneficial effect and is instead deleterious (Table 3). Thus, in addition to ligand field, 3*d* filling should also be considered as a factor in assessing the ideal admixture of HF exchange.

Table 3. Spin-state splitting and error (in parentheses) with respect to experiment for Ti(III), Fe(II), and Ni(II) ions in kcal/mol for representative functional choices: GGA, meta-GGA, 40% HF exchange, and meta-GGA with 40% HF exchange. These four choices correspond to the corners of the plot in Figure 7 for transition metal complexes. The method with the smallest error for each ion is indicated in bold.

Method	Ti(III)	Fe(II)	Ni(II)
GGA	-12.4	-96.7	-9.6
	(11.8)	(-10.0)	(30.3)
meta-GGA	-13.4	**-89.5**	-11.0
	(10.5)	**(-2.8)**	(28.9)
40% HF	-15.5	-105.4	-11.8
	(8.7)	(-18.7)	(28.1)
meta-GGA	**-16.8**	-98.2	**-13.3**
with 40% HF	**(7.4)**	(-11.5)	**(26.6)**

Opposing behavior of meta-GGA exchange depending on degree of metal-ligand bonding as indicated by these two cases should not necessarily discourage the use of meta-GGAs in transition metal chemistry. Close connections between functional behavior and degrees of chemical bonding do, however, motivate the use of strategies that interpolate across functional parameters, as we have previously done for both reaction coordinates[102] and variation in charge[45]. We have also recently found that functional behavior can be easily reproduced in transition metal complexes when a relatively sparse number of metal and ligand descriptors are employed (i.e., in the training of a neural network), suggesting it should be possible to use this same approach to identify optimal functional choice based on accurate benchmark results. Finally, comparison of delocalization errors in both the density and energetics[14] across ligand field strengths would

likely provide valuable insight into continued development of electronic structure methods for transition metal chemistry.

5. Conclusions

We have identified the effect of meta-GGA exchange on transition metal ion and octahedral complex spin-state properties through a tuning strategy we introduced to continually vary exchange enhancement factors from a GGA (i.e., PBE) to meta-GGA (i.e., TPSS) definition. We showed that meta-GGA exchange tuning reduced errors in some isolated ions by an order of magnitude but also increased some errors. The incorporation of meta-GGA exchange both stabilized and destabilized high-spin states in a manner more flexible than high-spin-biasing HF exchange tuning, but this effect was more limited on early- or late- transition metals than in mid-row ions.

For the transition-metal complexes, we observed a strongly ligand-field-dependent effect of meta-GGA exchange on spin-state ordering. For strong-field ligands (i.e., CO), meta-GGA exchange stabilized high-spin states, particularly for the d^5-d^7 configuration metals where the difference between HS and LS states correspond to population of two antibonding states not occupied in the latter. Conversely, meta-GGA exchange behavior in weak-field (i.e., H_2O or NH_3) ligands mirrored trends observed for the ions, leading to high-spin state destabilization that is maximal for mid-row transition metals. Qualitative and quantitative density differences explained the apparent ligand-field dependence of meta-GGA exchange behavior.

We confirmed that due to underlying GGA bias for low-spin states, a combined strategy of meta-GGA exchange incorporation within a hybrid functional should mandate high (i.e., > 30%) HF exchange for weak-field ligands, whereas meta-GGA exchange can nearly eliminate the need for HF exchange (i.e., < 10%) to reproduce accurate benchmark results on strong-field

ligands. This work should not discourage the use of meta-GGA exchange for the study of transition metal complexes, but it does highlight the degree to which the optimal functional choice depends on the underlying chemical bonding.

ASSOCIATED CONTENT

Supporting Information. Structures of all octahedral complexes; total or relative energies of transition metal ions (Ti^{2+}-Cu^{3+}) computed with variation of a modified TPSS functional and resulting slopes and correlation coefficients; results for Fe(II/III) phosphine complexes; density differences of Fe(II) complexes; SCAN relative high-spin/low-spin energetics compared to reference values and resulting errors on transition metal ions (Ti^{2+}-Cu^{3+}); comparison of SCAN, TPSS, and M06-L errors on select Fe(II) complexes; octahedral complex (with carbonyl, ammine, or aqua ligands) HS-LS total or relative energies computed with variation of a modified TPSS functional and resulting slopes and correlation coefficients; S^2 values of octahedral complex open shell singlets; discussion and visualization of correlation of meta-GGA exchange sensitivity with descriptors including charge differences, splittings, charge sensitivities, bond critical point characteristics. This material is available free of charge via the Internet at http://pubs.acs.org.

AUTHOR INFORMATION

Corresponding Author

*email: hjkulik@mit.edu phone: 617-253-4584

Notes

The authors declare no competing financial interest.

ACKNOWLEDGMENT

This work was supported by an MIT Energy Initiative seed grant. Partial support is also acknowledged from the National Science Foundation under grant number ECCS-1449291. H.J.K. holds a Career Award at the Scientific Interface from the Burroughs Wellcome Fund. This work was carried out in part using computational resources from the Extreme Science and Engineering Discovery Environment (XSEDE), which is supported by National Science Foundation grant number ACI-1053575. The authors thank Adam H. Steeves for providing a critical reading of the manuscript and illustrating the table of contents graphic.

References

1. Halcrow, M. A., Structure: Function Relationships in Molecular Spin-Crossover Complexes. *Chem. Soc. Rev.* **2011,** *40*, 4119-4142.
2. Létard, J.-F.; Guionneau, P.; Goux-Capes, L., Towards Spin Crossover Applications. In *Spin Crossover in Transition Metal Compounds III*, Springer: 2004; pp 221-249.
3. Harvey, J. N.; Poli, R.; Smith, K. M., Understanding the Reactivity of Transition Metal Complexes Involving Multiple Spin States. *Coord. Chem. Rev.* **2003,** *238*, 347-361.
4. Greeley, J.; Jaramillo, T. F.; Bonde, J.; Chorkendorff, I.; Nørskov, J. K., Computational High-Throughput Screening of Electrocatalytic Materials for Hydrogen Evolution. *Nat. Mater.* **2006,** *5*, 909-913.
5. Nørskov, J. K.; Bligaard, T.; Rossmeisl, J.; Christensen, C. H., Towards the Computational Design of Solid Catalysts. *Nat. Chem.* **2009,** *1*, 37-46.
6. Jensen, P. B.; Bialy, A.; Blanchard, D.; Lysgaard, S.; Reumert, A. K.; Quaade, U. J.; Vegge, T., Accelerated DFT-Based Design of Materials for Ammonia Storage. *Chem. Mater.* **2015,** *27*, 4552-4561.
7. Hautier, G.; Fischer, C. C.; Jain, A.; Mueller, T.; Ceder, G., Finding Nature's Missing Ternary Oxide Compounds Using Machine Learning and Density Functional Theory. *Chem. Mater.* **2010,** *22*, 3762-3767.
8. Jain, A.; Hautier, G.; Moore, C. J.; Ong, S. P.; Fischer, C. C.; Mueller, T.; Persson, K. A.; Ceder, G., A High-Throughput Infrastructure for Density Functional Theory Calculations. *Comput. Mater. Sci.* **2011,** *50*, 2295-2310.
9. Hautier, G.; Miglio, A.; Ceder, G.; Rignanese, G.-M.; Gonze, X., Identification and Design Principles of Low Hole Effective Mass P-Type Transparent Conducting Oxides. *Nat. Commun.* **2013,** *4*, 2292.
10. Gani, T. Z. H.; Ioannidis, E. I.; Kulik, H. J., Computational Discovery of Hydrogen Bond Design Rules for Electrochemical Ion Separation. *Chem. Mater.* **2016,** *28*, 6207-6218.

11. Bowman, D. N.; Bondarev, A.; Mukherjee, S.; Jakubikova, E., Tuning the Electronic Structure of Fe(II) Polypyridines via Donor Atom and Ligand Scaffold Modifications: A Computational Study. *Inorg. Chem.* **2015,** *54*, 8786-8793.
12. Cramer, C. J.; Truhlar, D. G., Density Functional Theory for Transition Metals and Transition Metal Chemistry. *Phys. Chem. Chem. Phys.* **2009,** *11*, 10757-10816.
13. Cohen, A. J.; Mori-Sánchez, P.; Yang, W., Insights into Current Limitations of Density Functional Theory. *Science* **2008,** *321*, 792-794.
14. Gani, T. Z. H.; Kulik, H. J., Where Does the Density Localize? Convergent Behavior for Global Hybrids, Range Separation, and DFT+U *J. Chem. Theory Comput.* **2016,** *12*, 5931-5945.
15. Burke, K., Perspective on Density Functional Theory. *J. Chem. Phys.* **2012,** *136*, 150901.
16. Becke, A. D., Perspective: Fifty Years of Density-Functional Theory in Chemical Physics. *J. Chem. Phys.* **2014,** *140*, 18A301.
17. Mortensen, S. R.; Kepp, K. P., Spin Propensities of Octahedral Complexes from Density Functional Theory. *J. Phys. Chem. A* **2015,** *119*, 4041-4050.
18. Ioannidis, E. I.; Kulik, H. J., Towards Quantifying the Role of Exact Exchange in Predictions of Transition Metal Complex Properties. *J. Chem. Phys.* **2015,** *143*, 034104.
19. Kulik, H. J., Perspective: Treating Electron Over-delocalization with the DFT+U Method. *J. Chem. Phys.* **2015,** *142*, 240901.
20. Janet, J. P.; Zhao, Q.; Ioannidis, E. I.; Kulik, H. J., Density Functional Theory for Modeling Large Molecular Adsorbate-Surface Interactions: A Mini-Review and Worked Example. *Mol. Sim.* **2016,** *in press,* http://dx.doi.org/10.1080/08927022.2016.1258465.
21. Droghetti, A.; Alfè, D.; Sanvito, S., Assessment of Density Functional Theory for Iron(II) Molecules across the Spin-Crossover Transition. *J. Chem. Phys.* **2012,** *137*, 124303.
22. Ganzenmüller, G.; Berkaïne, N.; Fouqueau, A.; Casida, M. E.; Reiher, M., Comparison of Density Functionals for Differences between the High- (T2g5) and Low- (A1g1) Spin States of Iron(II) Compounds. IV. Results for the Ferrous Complexes [Fe(L)('NHS4')]. *J. Chem. Phys.* **2005,** *122*, 234321.
23. Kepp, K. P., Theoretical Study of Spin Crossover in 30 Iron Complexes. *Inorg. Chem.* **2016,** *55*, 2717-2727.
24. Zein, S.; Borshch, S. A.; Fleurat-Lessard, P.; Casida, M. E.; Chermette, H., Assessment of the Exchange-Correlation Functionals for the Physical Description of Spin Transition Phenomena by Density Functional Theory Methods: All the Same? *J. Chem. Phys.* **2007,** *126*, 014105.
25. Boguslawski, K.; Jacob, C. R.; Reiher, M., Can DFT Accurately Predict Spin Densities? Analysis of Discrepancies in Iron Nitrosyl Complexes. *J. Chem. Theory Comput.* **2011,** *7*, 2740-2752.
26. Bleda, E. A.; Trindle, C.; Altun, Z., Studies on Spin State Preferences in Fe(II) Complexes. *Comput. Theor. Chem.* **2015,** *1073*, 139-148.
27. Milko, P.; Iron, M. A., On the Innocence of Bipyridine Ligands: How Well Do DFT Functionals Fare for These Challenging Spin Systems? *J. Chem. Theory Comput.* **2014,** *10*, 220-235.
28. Bowman, D. N.; Jakubikova, E., Low-Spin Versus High-Spin Ground State in Pseudo-Octahedral Iron Complexes. *Inorg. Chem.* **2012,** *51*, 6011-6019.
29. Reiher, M.; Salomon, O.; Hess, B. A., Reparameterization of Hybrid Functionals Based on Energy Differences of States of Different Multiplicity. *Theor. Chem. Acc.* **2001,** *107*, 48-55.

30. Reiher, M., Theoretical Study of the Fe(Phen)2(NCS)2 Spin-Crossover Complex with Reparametrized Density Functionals. *Inorg. Chem.* **2002,** *41*, 6928-6935.
31. Salomon, O.; Reiher, M.; Hess, B. A., Assertion and Validation of the Performance of the B3LYP* Functional for the First Transition Metal Row and the G2 Test Set. *J. Chem. Phys.* **2002,** *117*, 4729-4737.
32. Fouqueau, A.; Mer, S.; Casida, M. E.; Lawson Daku, L. M.; Hauser, A.; Mineva, T.; Neese, F., Comparison of Density Functionals for Energy and Structural Differences between the High- [5t2g:(T2g)4(Eg)2] and Low- [1a1g:(T2g)6(Eg)0] Spin States of the Hexaquoferrous Cation [Fe(H2O)6]2+. *J. Chem. Phys.* **2004,** *120*, 9473-9486.
33. Fouqueau, A.; Casida, M. E.; Lawson Daku, L. M.; Hauser, A.; Neese, F., Comparison of Density Functionals for Energy and Structural Differences between the High- [5t2g:(T2g)4(Eg)2] and Low- [1a1g:(T2g)6(Eg)0] Spin States of Iron(II) Coordination Compounds. II. More Functionals and the Hexaminoferrous Cation, [Fe(NH3)6]2+. *J. Chem. Phys.* **2005,** *122*, 044110.
34. Zhou, H.-C.; Long, J. R.; Yaghi, O. M., Introduction to Metal–Organic Frameworks. *Chem. Rev.* **2012,** *112*, 673-674.
35. Real, J. A.; Gaspar, A. B.; Muñoz, M. C., Thermal, Pressure and Light Switchable Spin-Crossover Materials. *Dalton Trans.* **2005**, 2062-2079.
36. Gaspar, A. B.; Ksenofontov, V.; Seredyuk, M.; Gütlich, P., Multifunctionality in Spin Crossover Materials. *Coord. Chem. Rev.* **2005,** *249*, 2661-2676.
37. Tarafder, K.; Kanungo, S.; Oppeneer, P. M.; Saha-Dasgupta, T., Pressure and Temperature Control of Spin-Switchable Metal-Organic Coordination Polymers from Ab Initio Calculations. *Phys. Rev. Lett.* **2012,** *109*, 077203.
38. Anisimov, V. I.; Zaanen, J.; Andersen, O. K., Band Theory and Mott Insulators: Hubbard U Instead of Stoner I. *Phys. Rev. B* **1991,** *44*, 943-954.
39. Liechtenstein, A. I.; Anisimov, V. I.; Zaanen, J., Density-Functional Theory and Strong-Interactions - Orbital Ordering in Mott-Hubbard Insulators. *Phys. Rev. B* **1995,** *52*, R5467-R5470.
40. Dudarev, S. L.; Botton, G. A.; Savrasov, S. Y.; Humphreys, C. J.; Sutton, A. P., Electron-Energy-Loss Spectra and the Structural Stability of Nickel Oxide: An LSDA+U Study. *Phys. Rev. B* **1998,** *57*, 1505-1509.
41. Kulik, H. J.; Marzari, N., Systematic Study of First-Row Transition-Metal Diatomic Molecules: A Self-Consistent DFT Plus U Approach. *J. Chem. Phys.* **2010,** *133*, 114103.
42. Kulik, H. J.; Marzari, N., A Self-Consistent Hubbard U Density-Functional Theory Approach to the Addition-Elimination Reactions of Hydrocarbons on Bare FeO+. *J. Chem. Phys.* **2008,** *129*, 134314.
43. Kulik, H. J.; Cococcioni, M.; Scherlis, D. A.; Marzari, N., Density Functional Theory in Transition-Metal Chemistry: A Self-Consistent Hubbard U Approach. *Phys. Rev. Lett.* **2006,** *97*, 103001.
44. Cococcioni, M.; de Gironcoli, S., Linear Response Approach to the Calculation of the Effective Interaction Parameters in the LDA+U Method. *Phys. Rev. B* **2005,** *71*, 035105.
45. Zhao, Q.; Ioannidis, E. I.; Kulik, H. J., Global and Local Curvature in Density Functional Theory. *J. Chem. Phys.* **2016,** *145*, 054109.
46. Della Sala, F.; Fabiano, E.; Constantin, L. A., Kinetic-Energy-Density Dependent Semilocal Exchange-Correlation Functionals. *Int. J. Quantum Chem.* **2016,** *116*, 1641-1694.

47. Furche, F.; Perdew, J. P., The Performance of Semilocal and Hybrid Density Functionals in 3d Transition-Metal Chemistry. *J. Chem. Phys.* **2006,** *124*, 044103.
48. Zhao, Y.; Truhlar, D. G., The M06 Suite of Density Functionals for Main Group Thermochemistry, Thermochemical Kinetics, Noncovalent Interactions, Excited States, and Transition Elements: Two New Functionals and Systematic Testing of Four M06-Class Functionals and 12 Other Functionals. *Theor. Chem. Acc.* **2008,** *120*, 215-241.
49. Swart, M.; Groenhof, A. R.; Ehlers, A. W.; Lammertsma, K., Validation of Exchange–Correlation Functionals for Spin States of Iron Complexes. *J. Phys. Chem. A* **2004,** *108*, 5479-5483.
50. Shil, S.; Bhattacharya, D.; Sarkar, S.; Misra, A., Performance of the Widely Used Minnesota Density Functionals for the Prediction of Heat of Formations, Ionization Potentials of Some Benchmarked First Row Transition Metal Complexes. *J. Phys. Chem. A* **2013,** *117*, 4945-4955.
51. Huang, W.; Xing, D.-H.; Lu, J.-B.; Long, B.; Schwarz, W. E.; Li, J., How Much Can Density Functional Approximations (DFA) Fail? The Extreme Case of the FeO4 Species. *J. Chem. Theory Comput.* **2016,** *12*, 1525-1533.
52. Tao, J.; Perdew, J. P.; Staroverov, V. N.; Scuseria, G. E., Climbing the Density Functional Ladder: Nonempirical Meta-Generalized Gradient Approximation Designed for Molecules and Solids. *Phys. Rev. Lett.* **2003,** *91*, 146401.
53. Sun, J.; Ruzsinszky, A.; Perdew, J. P., Strongly Constrained and Appropriately Normed Semilocal Density Functional. *Phys. Rev. Lett.* **2015,** *115*, 036402.
54. Kitchaev, D. A.; Peng, H.; Liu, Y.; Sun, J.; Perdew, J. P.; Ceder, G., Energetics of MnO2 Polymorphs in Density Functional Theory. *Phys. Rev. B* **2016,** *93*, 045132.
55. Fajín, J. L.; Viñes, F.; DS Cordeiro, M. N. l.; Illas, F.; Gomes, J. R., Effect of the Exchange-Correlation Potential on the Transferability of Brønsted–Evans–Polanyi Relationships in Heterogeneous Catalysis. *J. Chem. Theory Comput.* **2016,** *12*, 2121-2126.
56. Tran, F.; Stelzl, J.; Blaha, P., Rungs 1 to 4 of DFT Jacob's Ladder: Extensive Test on the Lattice Constant, Bulk Modulus, and Cohesive Energy of Solids. *J. Chem. Phys.* **2016,** *144*, 204120.
57. Wang, J.; Liu, L.; Wilson, A. K., Oxidative Cleavage of the β-O-4 Linkage of Lignin by Transition Metals: Catalytic Properties and the Performance of Density Functionals. *J. Phys. Chem. A* **2016,** *120*, 737-746.
58. Minenkov, Y.; Chermak, E.; Cavallo, L., Troubles in the Systematic Prediction of Transition Metal Thermochemistry with Contemporary out-of-the-Box Methods. *J. Chem. Theory Comput.* **2016,** *12*, 1542-1560.
59. Fang, Z.; Both, J.; Li, S.; Yue, S.; Aprà, E.; Keçeli, M.; Wagner, A. F.; Dixon, D. A., Benchmark Calculations of Energetic Properties of Groups 4 and 6 Transition Metal Oxide Nanoclusters Including Comparison to Density Functional Theory. *J. Chem. Theory Comput.* **2016,** *12*, 3689-3710.
60. Coskun, D.; Jerome, S. V.; Friesner, R. A., Evaluation of the Performance of the B3LYP, PBE0, and M06 DFT Functionals, and DBLOC-Corrected Versions, in the Calculation of Redox Potentials and Spin Splittings for Transition Metal Containing Systems. *J. Chem. Theory Comput.* **2016,** *12*, 1121-1128.
61. Ye, S.; Neese, F., Accurate Modeling of Spin-State Energetics in Spin-Crossover Systems with Modern Density Functional Theory. *Inorg. Chem.* **2010,** *49*, 772-774.

62. Vancoillie, S.; Zhao, H.; Radoń, M.; Pierloot, K., Performance of CASPT2 and DFT for Relative Spin-State Energetics of Heme Models. *J. Chem. Theory Comput.* **2010,** *6*, 576-582.
63. Jensen, K. P.; Cirera, J., Accurate Computed Enthalpies of Spin Crossover in Iron and Cobalt Complexes. *J. Phys. Chem. A* **2009,** *113*, 10033-10039.
64. Bühl, M.; Reimann, C.; Pantazis, D. A.; Bredow, T.; Neese, F., Geometries of Third-Row Transition-Metal Complexes from Density-Functional Theory. *J. Chem. Theory Comput.* **2008,** *4*, 1449-1459.
65. Jensen, K. P.; Roos, B. O.; Ryde, U., Performance of Density Functionals for First Row Transition Metal Systems. *J. Chem. Phys.* **2007,** *126*, 014103.
66. Jensen, K. P., Bioinorganic Chemistry Modeled with the TPSSh Density Functional. *Inorg. Chem.* **2008,** *47*, 10357-10365.
67. Riley, K. E.; Merz, K. M., Assessment of Density Functional Theory Methods for the Computation of Heats of Formation and Ionization Potentials of Systems Containing Third Row Transition Metals. *J. Phys. Chem. A* **2007,** *111*, 6044-6053.
68. Perdew, J. P.; Burke, K.; Ernzerhof, M., Generalized Gradient Approximation Made Simple. *Phys. Rev. Lett.* **1996,** *77*, 3865-3868.
69. Moroni, S.; Ceperley, D. M.; Senatore, G., Static Response and Local Field Factor of the Electron Gas. *Phys. Rev. Lett.* **1995,** *75*, 689-692.
70. Lieb, E. H.; Oxford, S., Improved Lower Bound on the Indirect Coulomb Energy. *Int. J. Quantum Chem.* **1981,** *19*, 427-439.
71. Perdew, J. P.; Ruzsinszky, A.; Tao, J.; Csonka, G. I.; Scuseria, G. E., One-Parameter Optimization of a Nonempirical Meta-Generalized-Gradient-Approximation for the Exchange-Correlation Energy. *Phys. Rev. A* **2007,** *76*, 042506.
72. Oyeyemi, V. B.; Keith, J. A.; Pavone, M.; Carter, E. A., Insufficient Hartree–Fock Exchange in Hybrid DFT Functionals Produces Bent Alkynyl Radical Structures. *J. Phys. Chem. Lett.* **2012,** *3*, 289-293.
73. Kramida, A.; Ralchenko, Y.; Reader, J.; Team, N. A., NIST Atomic Spectra Database (Ver. 5.3). National Institute of Standards and Technology, Gaithersburg, MD: 2015.
74. Schmidt, M. W.; Baldridge, K. K.; Boatz, J. A.; Elbert, S. T.; Gordon, M. S.; Jensen, J. H.; Koseki, S.; Matsunaga, N.; Nguyen, K. A.; Su, S., et al., General Atomic and Molecular Electronic Structure System. *J. Comput. Chem.* **1993,** *14*, 1347-1363.
75. Dunning, T. H., Gaussian Basis Sets for Use in Correlated Molecular Calculations. I. The Atoms Boron through Neon and Hydrogen. *J. Chem. Phys.* **1989,** *90*, 1007-1023.
76. Ioannidis, E. I.; Gani, T. Z. H.; Kulik, H. J., Molsimplify: A Toolkit for Automating Discovery in Inorganic Chemistry. *J. Comput. Chem.* **2016,** *37*, 2106-2117.
77. Ditchfield, R.; Hehre, W. J.; Pople, J. A., Self-Consistent Molecular-Orbital Methods. IX. An Extended Gaussian-Type Basis for Molecular-Orbital Studies of Organic Molecules. *J. Chem. Phys.* **1971,** *54*, 724-728.
78. Weigend, F.; Ahlrichs, R., Balanced Basis Sets of Split Valence, Triple Zeta Valence and Quadruple Zeta Valence Quality for H to Rn: Design and Assessment of Accuracy. *Phys. Chem. Chem. Phys.* **2005,** *7*, 3297-3305.
79. E. D. Glendening, J., K. Badenhoop, A. E. Reed, J. E. Carpenter, J. A. Bohmann, C. M. Morales, C. R. Landis, and F. Weinhold, NBO, Version 6.0. 2013.
80. Bader, R. F., A Quantum Theory of Molecular Structure and Its Applications. *Chem. Rev.* **1991,** *91*, 893-928.

81. Lu, T.; Chen, F., Multiwfn: A Multifunctional Wavefunction Analyzer. *J. Comput. Chem.* **2012,** *33*, 580-592.
82. Andersson, K.; Malmqvist, P. Å.; Roos, B. O., Second-Order Perturbation Theory with a Complete Active Space Self-Consistent Field Reference Function. *J. Chem. Phys.* **1992,** *96*, 1218-1226.
83. Aquilante, F.; Autschbach, J.; Carlson, R. K.; Chibotaru, L. F.; Delcey, M. G.; De Vico, L.; Ferré, N.; Frutos, L. M.; Gagliardi, L.; Garavelli, M., Molcas 8: New Capabilities for Multiconfigurational Quantum Chemical Calculations across the Periodic Table. *J. Comput. Chem.* **2016,** *37*, 506-541.
84. Roos, B. O.; Lindh, R.; Malmqvist, P.-Å.; Veryazov, V.; Widmark, P.-O., New Relativistic Ano Basis Sets for Transition Metal Atoms. *J. Phys. Chem. A* **2005,** *109*, 6575-6579.
85. Roos, B. O.; Lindh, R.; Malmqvist, P.-Å.; Veryazov, V.; Widmark, P.-O., Main Group Atoms and Dimers Studied with a New Relativistic Ano Basis Set. *J. Phys. Chem. A* **2004,** *108*, 2851-2858.
86. Douglas, M.; Kroll, N. M., Quantum Electrodynamical Corrections to the Fine Structure of Helium. *Ann. Phys.* **1974,** *82*, 89-155.
87. Hess, B. A., Relativistic Electronic-Structure Calculations Employing a Two-Component No-Pair Formalism with External-Field Projection Operators. *Phys. Rev. A* **1986,** *33*, 3742.
88. Forsberg, N.; Malmqvist, P.-Å., Multiconfiguration Perturbation Theory with Imaginary Level Shift. *Chem. Phys. Lett.* **1997,** *274*, 196-204.
89. Ghigo, G.; Roos, B. O.; Malmqvist, P.-A., A Modified Definition of the Zeroth-Order Hamiltonian in Multiconfigurational Perturbation Theory (CASPT2). *Chem. Phys. Lett.* **2004,** *396*, 142-149.
90. Bolvin, H., d→ d Spectrum and High-Spin/Low-Spin Competition in D6 Octahedral Coordination Compounds: Ab Initio Study of Potential Energy Curves. *J. Phys. Chem. A* **1998,** *102*, 7525-7534.
91. Domingo, A.; Àngels Carvajal, M.; de Graaf, C., Spin Crossover in Fe(II) Complexes: An Ab Initio Study of Ligand σ-Donation. *Int. J. Quantum Chem.* **2010,** *110*, 331-337.
92. Pierloot, K.; Vancoillie, S., Relative Energy of the High-(T2g5) and Low-(A1g1) Spin States of [Fe(H2O)6]2+, [Fe(NH3)6]2+, and [Fe(Bpy)3]2+: CASPT2 Versus Density Functional Theory. *J. Chem. Phys.* **2006,** *125*, 124303.
93. Sousa, C.; de Graaf, C., Ab Initio Wavefunction Approaches to Spin States. In *Spin States in Biochemistry and Inorganic Chemistry*, John Wiley & Sons, Ltd: 2015; pp 35-57.
94. Perdew, J. P.; Tao, J.; Staroverov, V. N.; Scuseria, G. E., Meta-Generalized Gradient Approximation: Explanation of a Realistic Nonempirical Density Functional. *J. Chem. Phys.* **2004,** *120*, 6898-6911.
95. Becke, A. D., A New Mixing of Hartree–Fock and Local Density-Functional Theories. *J. Chem. Phys.* **1993,** *98*, 1372-1377.
96. Adamo, C.; Barone, V., Toward Reliable Density Functional Methods without Adjustable Parameters: The PBE0 Model. *J. Chem. Phys.* **1999,** *110*, 6158-6170.
97. Becke, A. D., Density-Functional Thermochemistry. V. Systematic Optimization of Exchange-Correlation Functionals. *J. Chem. Phys.* **1997,** *107*, 8554-8560.
98. Zhao, Y.; Truhlar, D. G., Exploring the Limit of Accuracy of the Global Hybrid Meta Density Functional for Main-Group Thermochemistry, Kinetics, and Noncovalent Interactions. *J. Chem. Theory Comput.* **2008,** *4*, 1849-1868.

99. Zhao, Y.; Schultz, N. E.; Truhlar, D. G., Design of Density Functionals by Combining the Method of Constraint Satisfaction with Parametrization for Thermochemistry, Thermochemical Kinetics, and Noncovalent Interactions. *J. Chem. Theory Comput.* **2006,** *2*, 364-382.
100. Staroverov, V. N.; Scuseria, G. E.; Tao, J.; Perdew, J. P., Comparative Assessment of a New Nonempirical Density Functional: Molecules and Hydrogen-Bonded Complexes. *J. Chem. Phys.* **2003,** *119*, 12129-12137.
101. Zhao, Y.; Schultz, N. E.; Truhlar, D. G., Exchange-Correlation Functional with Broad Accuracy for Metallic and Nonmetallic Compounds, Kinetics, and Noncovalent Interactions. *J. Chem. Phys.* **2005,** *123*, 161103.
102. Kulik, H. J.; Marzari, N., Accurate Potential Energy Surfaces with a DFT+U(R) Approach. *J. Chem. Phys.* **2011,** *135*, 194105.

TOC graphic